STYRELSEN FÖR

VINTERSJÖFARTSFORSKNING

WINTER NAVIGATION RESEARCH BOARD

Research Report No 32

STATISTICAL FEATURES OF SEA ICE RIDGING IN THE GULF OF BOTHNIA

BY MATTI LEPPÄRANTA

Sjöfartsstyrelsen
Finland

Finnish Board of Navigation

Sjöfartsverket
Sverige

Swedish Administration
of Shipping and Navigation

STATISTICAL FEATURES OF SEA ICE RIDGING IN THE GULF OF BOTHNIA

Matti Leppäranta
Institute of Marine Research
P.O. Box 166
SF-00141 Helsinki 14
Finland

ISBN 951-46-5105-7

Helsinki 1981. Government Printing Centre

FOREWORD

The winter Navigation Research Board presents its report No 32. This is an account of a study of ice ridge sail heights and ridge distribution in the Gulf of Bothnia in the winter 1979. The exercise not only produced additional knowledge about ridges but gave also valuable experience of the observation method: a shipborne laser profilometer was used.

The winter Navigation Research Board expresses its thanks to Mr. Leppäranta and his Colleaques and to all those, who have assisted in this work.

Helsinki and Norrköping, November 1980.

Jan-Erik Jansson

Lennart Johansson

CONTENTS

Abstract

Spatial distributions of ridge sail heights and ridge spacings in the Gulf of Bothnia are studied. Observations have been made with a laser-profilometer from an ice-breaker deck during two series of experiments in the winter of 1979. Errors due to the influence of ridged ice field on the ship and due to averaging over finite distances are discussed. Measured tracks are on an average 10 km long. Mean sail height varies between 38 and 67 cm and ridge density between 2.1 and 22.1/km, the cutoff height for sails being 30 cm. Both sail heights and ridge spacings fit well with an exponential distribution, but use of this for sail heights leads to underestimation of the density of large ridges. The mass of ridged ice is 4-62 cm in terms of equivalent ice thickness; in one case the mass of ridged ice exceeded the mass of level ice along the track. Sensitivity of the results to the choice of the cutoff height is discussed.

1. INTRODUCTION

This work is concerned with the distribution of ice ridge size and density in the Gulf of Bothnia. The idea for this research originated with Professor Erkki Palosuo, former Head of the Department of Geophysics at the University of Helsinki, and it is a continuation of his detailed studies on the formation and structure of Baltic sea ice ridges. The method of observations had been developed by Prof. Palosuo, who has also actively participated in analysing the results (PALOSUO & LEPPÄRANTA 1979).

Background

The sea ice ridges which occur every winter in the Baltic Sea constitute a severe problem to winter navigation. Extensive research on Baltic ridges began in the late 1960's, first concentrating on the formation and structure of single ridges (PALOSUO 1975). It was recognized that data on spatial distribution of size and density of ridges were needed and to obtain such data a laser-profilometer was acquired at the beginning of 1977 (PALOSUO 1977). This method had been already put to use in the Arctic Ocean a few years earlier (e.g. KETCHUM 1971, WEEKS et al. 1971).

The profilometer was first installed in a helicopter. The results showed that to get satisfactory data the helicopter should fly not faster than ~10 m/s (a restriction due to the properties of the profilometer). Thus it is not very economic to use a helicopter and attempts to take measurements from an ice-breaker deck, while the ice-breaker is performing her routine assistance work, were started in the winter 1977/78. During the winter that followed the research continued. The results were promising and operative use of the profilometer from an ice-breaker deck began in the winter of 1979/80.

The profilometer is used for studying floating sea ice ridges only and hence in this report only such ridges are considered. However, it should be noted that even in the open Baltic Sea there are shallow places where grounded ridges are observed every winter; these must be the object of a different type of study.

Structure of Baltic ice ridges

Geometry. Measurements of several ridge profiles in the Baltic Sea are given in PALOSUO (1975). It is seen that profile geometry is rather well approximated by a triangular shape for both the sail and the keel (Fig. 1). Most of the ridges measured by Palosuo have the basic geometric parameters as defined in Fig. 1 falling within the ranges:

sail height	h_s	½-2 m
sail inclination	ϕ	10-50°
keel depth	h_k	3-15 m
keel inclination	θ	30-60°

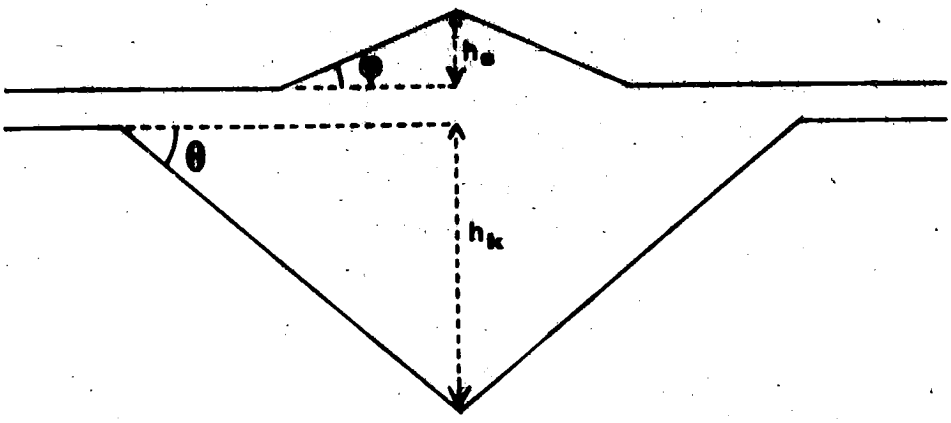

Figure 1. Idealized cross-sectional profile of a ridge.

The size of the ridges much depended on the thickness of level ice at the time of ridge formation. The ranges of sail height and keel depth given above correspond to a thickness interval of 20-80 cm.

The profilometer results presented below show that the above sail heights belong to the higher than average portion of typical sail height distribution. The largest ridge in PALOSUO (1975) had a sail height of 3.4 m and a keel kepth of 28 m, which is the largest ever recorded in the Baltic Sea.

Internal structure. The ice blocks in the sail and keel are loose or only lightly frozen together and the totally frozen layer never extends to more than one meter depth below the water-line (PALOSUO 1975). KEINONEN (1977) made a detailed study on ridge sails and observed that most of the space between ice blocks is filled with snow. The relative volume of air and snow in sails was 0.36 - 0.43. The density of ice blocks in the sail was 0.87 Mgm^{-3}, while the density of level ice near the ridges was 0.915 Mgm^{-3}. The density of snow on Baltic Sea ice is 0.2 - 0.45 Mgm^{-3} (LEPPÄRANTA 1979, KEINONEN 1977).

Formation of Baltic ice ridges

Ridging in the Baltic Sea is caused by the wind. The size of the ridges formed depends on the wind speed, fetch, ice strength and ice thickness. Usually ridges can't form from thin ice. Thus, PARMERTER (1975) gives a theoretical estimate of 17 cm for minimum ridging thickness in the Arctic; PALOSUO (1975) reports one ridge formed from ice with thickness less than 15 cm.

For a fixed ice strength and thickness there is a limiting size to which ridges can grow, as was well demonstrated by PARMERTER & COON (1972) using a theoretical pressure ridging model. Application of the model to Baltic ice conditions (LEPPÄRANTA 1977) showed that the theoretical limiting size was close to the size of the large ridges measured by PALOSUO (1975) (Fig. 2). The theoretical limiting size tended to be smaller, due to using the value zero for porosity of ridges in the calculations.

The shape of the ridges depends strongly on the mode of deformation during ridging (WEEKS et al. 1971, PALOSUO 1975). Shear ridges tend to have steeper inclination angles than pressure ridges and the broken ice blocks become smaller under shear.

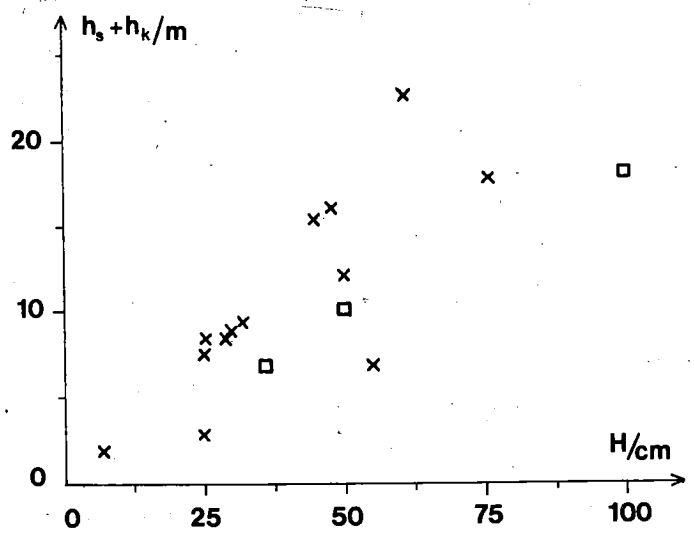

Figure 2. Total height of large ridges versus ice sheet thickness; × - observations of PALOSUO (1975), □ - calculations with Parmerter-Coon model (LEPPÄRANTA 1977).

Spatial distribution of Baltic ice ridges

It is shown below that the sail height distributions in the Baltic Sea fit well the exponential distribution proposed by WADHAMS (1979). Hence the amount of ridging observed is strongly dependent on the definition of a "ridge", i.e. on the cutoff height. Visual observations from a helicopter at the end of March 1977 in the Bothnian Bay gave an average ridge density of 7.5 km^{-1} (LEPPÄRANTA 1979), which agrees well with the profilometer results in this work, when a cutoff height of 30 cm is used. LEPPÄRANTA (1979) also observed that the ridge density is not significantly different in two mutually perpendicular directions.

Necessity of the profilometer observations

Important ridge parameters that influence a ship's capacity to penetrate a ridged ice field are (MÄKINEN et al. 1976):

1a. cross-sectional profile (amount of ice),

1b. block size,

1c. degree of freezing,

1d. thickness of snow cover,

2. distance between adjacent ridges.

With the profilometer, parameter 2 can be measured directly. Parameters 1a-d can be determined from a detailed study of an individual ridge. 1a can, however, be estimated from the sail profile given by the profilometer on the basis of the known physical properties of ridges. Finally, it is possible to estimate visually the thickness of snow (1d), when profilometer measurements are made from an ice-breaker.

There is scientific interest in the ridge data. The amount of ridging in different conditions is connected with the large-scale stress-strain relationship in the sea ice cover, which has been extensively studied over the last ten years.

Operative use of the profilometer will give input and verification data to numerical models for forecasting sea ice drift and deformation in the Baltic Sea. A model which has been operatively used in Finland since the winter of 1976/77 (LEPPÄRANTA 1980), gives a forecast for mean ridge size and ridge density, quantities which hitherto could only be qualitatively verified. In addition, the profilometer data can be used to predict more accurately the air stress on ice by including the form drag due to ridges (ARYA 1973). Naturally, then, the form drag in the water due to ridge keels can also be estimated.

2. THE METHOD OF MEASUREMENT

The profilometer

The profilometer is an impulse laser EUMIG LASER-RADAR LD151 HS made in Austria (Fig. 3). It sends infra-red (wavelength 903 nm) impulses with 300 Hz frequency and beam divergence 1.4 mrad. The operational scheme is shown in Fig. 4.

The time-measuring unit calculates one hundred distance values and gives their mean as a measured distance in BCD format to the magnetic cassette and the value is also shown in the digital display. The time interval t_p between two successive measurements is 1/3 seconds (the exact experimentally determined value is 0.359 s).

The magnetic cassette is later read into the computer in the Institute of Marine Research in Helsinki, where the data are analyzed.

The laser can measure distances up to 40 or 120 m, if the reflecting surface is matt dark or matt light, respectively. According to the manufactorer, the accuracy is $\pm$ 10 cm $\pm$ $10^{-3} \cdot d$, where d is the measured value.

Figure 3. (a) The path through an ice field broken by the ice-breaker Urho, (b) the profilometer installed on the deck, of Urho,

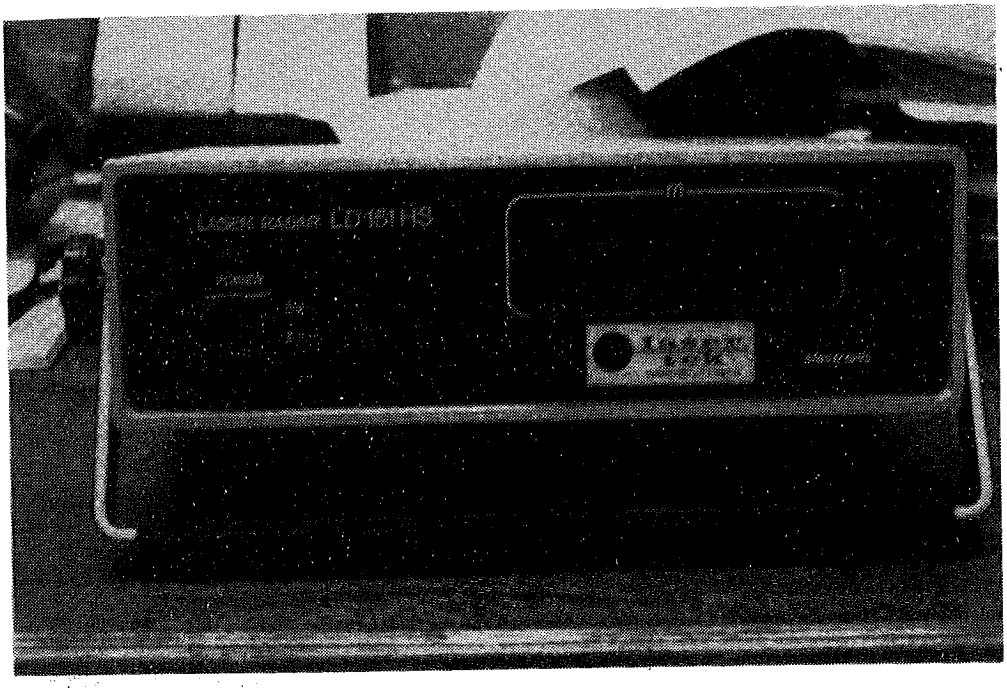

Figure 3. (cont.). (c) the digital display, and (d) the magnetic cassette recorder

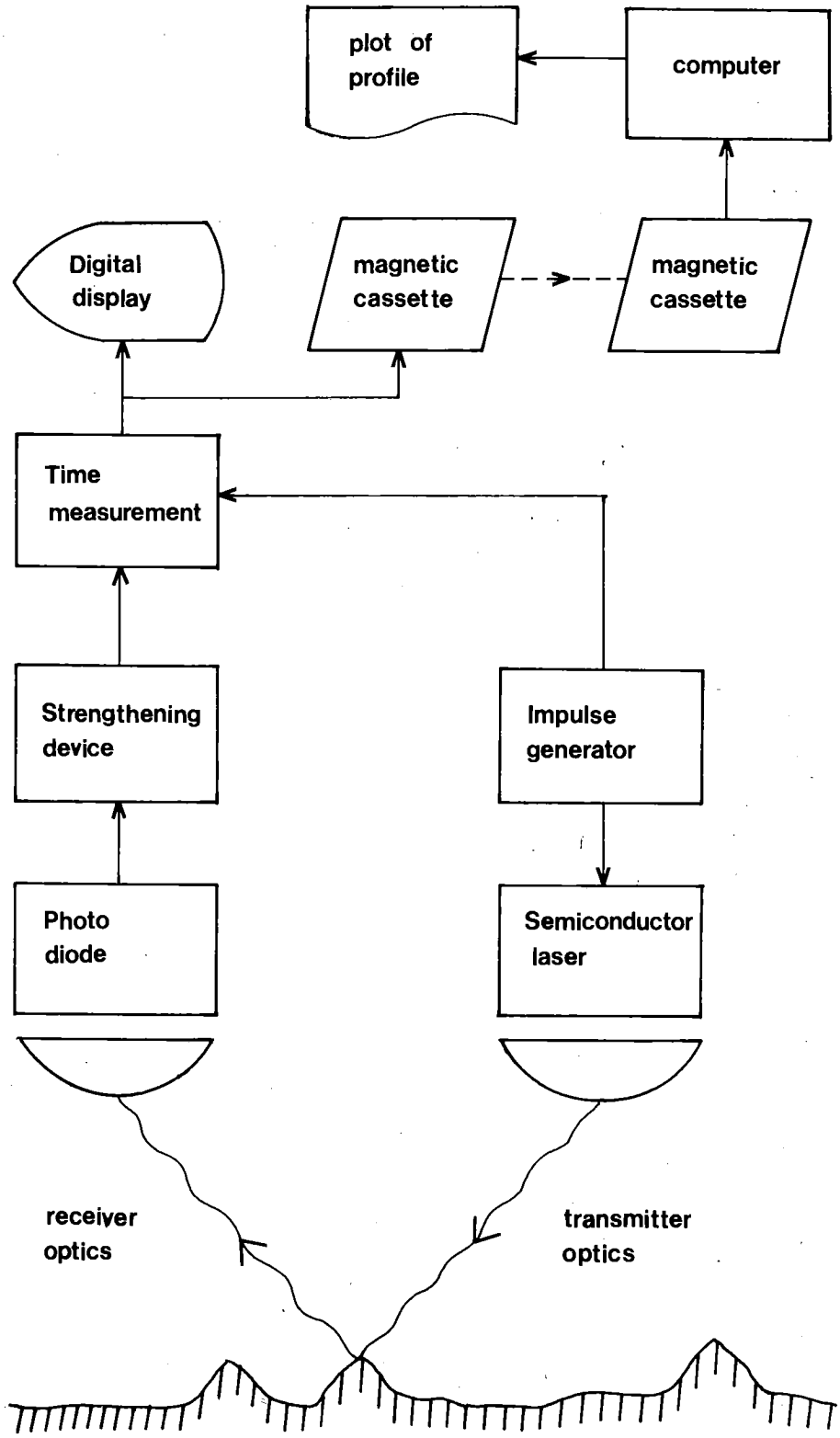

Figure 4. The operational scheme of the measurement system.

Installation

The profilometer is installed on the deck of an ice-breaker so that the laser-beam makes an angle of β = 47.5 degrees with the vertical (Fig. 5). The altitude of the profilometer above level ice being 16 m, the measured distances are then 23 m (= 16 m/ cos β) for level ice and 20-23 m for ridges.

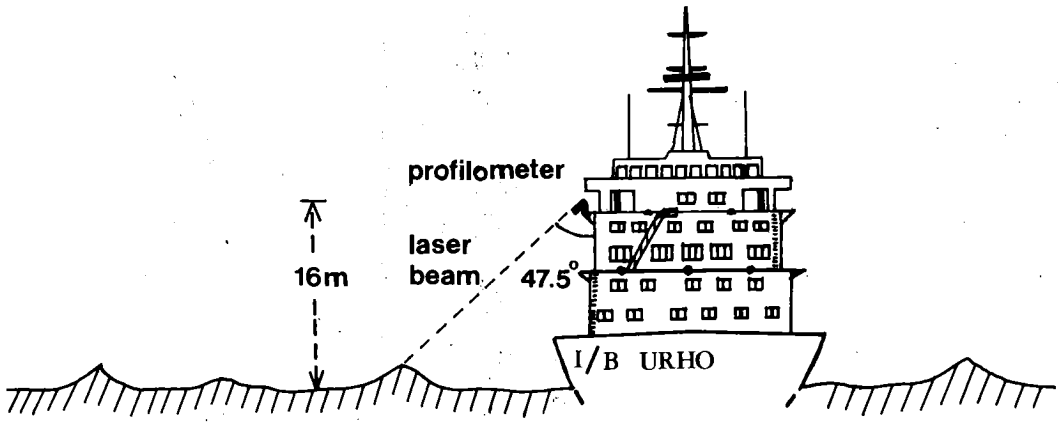

Figure 5. Installation of the profilometer on the ice-breaker URHO.

Data recording

The profilometer integrates mean distances over a path l_p, the length of which depends on the speed of the ice-breaker, v:

$$l_p = v\, t_p \ .$$

A typical value for v is 10 knots (5.1 ms^{-1}) and in general can vary between 5 and 15 knots (2.6 and 7.7 ms^{-1}) depending on ice conditions and on the ability of the assisted ships to follow the ice-breaker. t_p is the fixed profilometer constant (0.359 s). Hence l_p = 0.92, 1.85 or 2.76 m for v = 5, 10 or 15 knots, respectively.

The recording time for each surface profile is half an hour (one side of a cassette). With v = 10 knots the total path

length thus becomes 9.26 km. The speed v is considered constant for each profile. This is a good approximation, except that every time the ship penetrates a ridge her speed slows down; thus an error is introduced as regards ridge intervals, especially in the high frequency band of the spatial spectrum. It is hoped that this effect can be eliminated in the future.

The track of the ice-breaker during recording must be a straight line. Generally it is. However, if something unexpected happens, e.g. the ice-breaker must turn around to help a ship stuck in the ice field, the profiling must be suspended and recontinued when the course is once again straight. During the measurements reported in this work such interruptions occurred for three profiles only.

The actual and measured sail heights

The actual sail height of a ridge is, by definition, the maximum elevation of the ridge above a reference surface. In the present case it is convenient to choose this latter as the level surface in the neighbourhood of the ridge. Thus the definition corresponds to the visual image seen from above. The measured sail height, on the other hand, is the oblique (Fig. 5) distance from the laser to the level surface minus the minimum oblique distance value given by the profilometer when passing the ridge.

The actual and measured sail heights are denoted by h_s and h_p, respectively. There are three factors which influence the deviation of h_p from h_s:

(i) the inclination of the laser-beam,
(ii) the averaging over the inverval l_p,
(iii) the buoyancy effect of ridges on the ship.

The first factor tends to make the measured value larger than the actual value, while the other two factors work in the opposite direction. In this section, these three factors are

first treated separately, i.e. equations for h_p/h_s are derived considering the factors one at the time, and then a general equation is given.

(i) The inclination angle β = 47.5 degrees (Fig. 5) introduces a factor of $1/\cos\beta$ in the distance differences. Thus,

$$\frac{h_p}{h_s} = \frac{1}{\cos\beta} \approx 1.48 \quad . \tag{2.1}$$

(ii) The effect of averaging can be derived mathematically (Fig. 6). The coordinate system is fixed so that the x-axis follows the level ice surface and the z-axis goes through the top of the sail. The model sail is symmetric and its width is $2 \cdot l_s$.

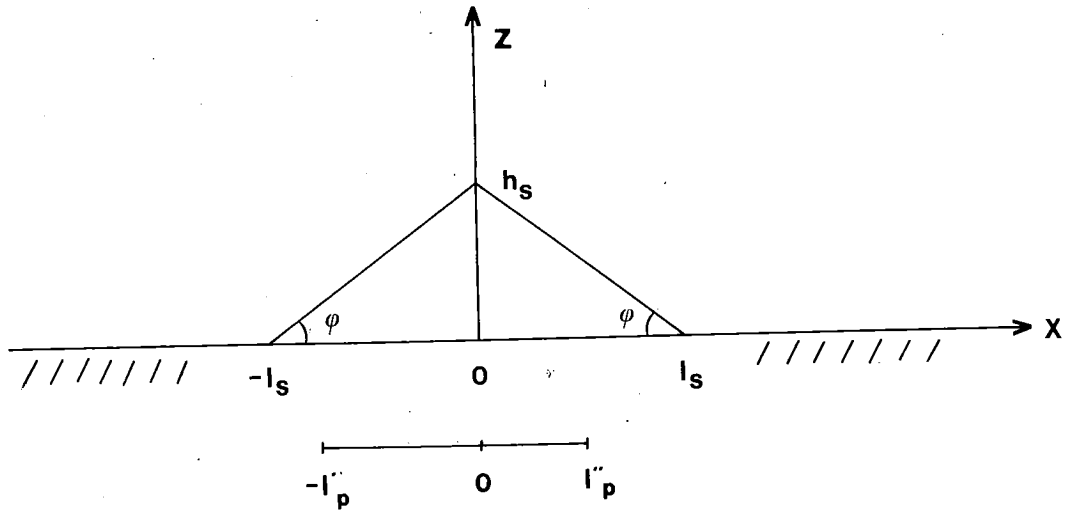

Figure 6. Integration of the ridge height by the profilometer: h_s - the actual sail height, l_s - half of the sail width, $l_p = l'_p + l''_p$ - the integration interval which gives the maximum integrated height.

The integration interval l_p corresponding to h_p must include the origin, i.e. the interval is of the form

$$-l'_p \leq x \leq l''_p \quad ,$$

where l'_p , $l''_p \geq 0$ and $l'_p + l''_p = l_p$, and thus

$$\frac{h_p}{h_s} = \frac{1}{h_s} \cdot \frac{1}{l_p} \int_{-l'_p}^{l''_p} z\,dx \quad . \tag{2.2}$$

A further simplication is made by assuming that $l_p \leq l_s$, which is equivalent to l'_p , $l''_p \leq l_s$ for any choice of l'_p and l''_p . This is a realistic assumption, since the ship's speed decreases when going through a ridge, thus reducing l_p to less than $\approx 1\frac{1}{2}$ m and, on the other hand, low ridges near the cutoff height tend to have small inclination angles which increases the ratio l_s/h_s (Fig. 7); for the cutoff height of 30 cm used in the present work, ϕ is less than $\approx 15^{\circ}$, which makes l_s greater than ≈ 1.2 m.

With the condition $l_p \leq l_s$, integration of (2.2) yields

$$\frac{h_p}{h_s} = \frac{l'_p}{l_p} \cdot \left\{ 1 - \tfrac{1}{2} \cdot \frac{l'_p}{l_s} \right\} + \left\{ 1 - \frac{l'_p}{l_p} \right\} \cdot \left\{ 1 - \tfrac{1}{2} \cdot \frac{l_p - l'_p}{l_s} \right\} \quad . \tag{2.3}$$

Since the lower limit of integration $-l'_p$ is not known, but can vary randomly between $-l_p$ and 0, equation (2.3) must be integrated to obtain the expectation value:

$$\left\langle \frac{h_p}{h_s} \right\rangle = \frac{1}{l_p} \int_{-l_p}^{0} \frac{h_p}{h_s}\, dl'_p = 1 - \frac{1}{3} \cdot \frac{l_p}{l_s} \quad . \tag{2.4}$$

Hence the relative reduction due to averaging is less than 1/3. The ratio l_p/l_s decreases and hence $\langle h_p/h_s \rangle$ increases with sail height.

(iii) The ridge buoyancy lifts the ship and reduces the measured distance differences (i.e. the altitude of the profilometer is higher when going through ridges than when going through level ice).

Formally,

$$\frac{h_p}{h_s} = B \quad , \tag{2.5}$$

where B is a dimensionless buoyancy correction, $B = B(h_s) \leq 1$ and B decreases with increasing h_s.

Combining now eqs. (2.1), (2.4) and (2.5) the final equation for $< h_p/h_s >$ is obtained:

$$< \frac{h_p}{h_s} > = \frac{B}{\cos \beta} \left(1 - \frac{1}{3} \cdot \frac{l_p}{l_s}\right) . \tag{2.6}$$

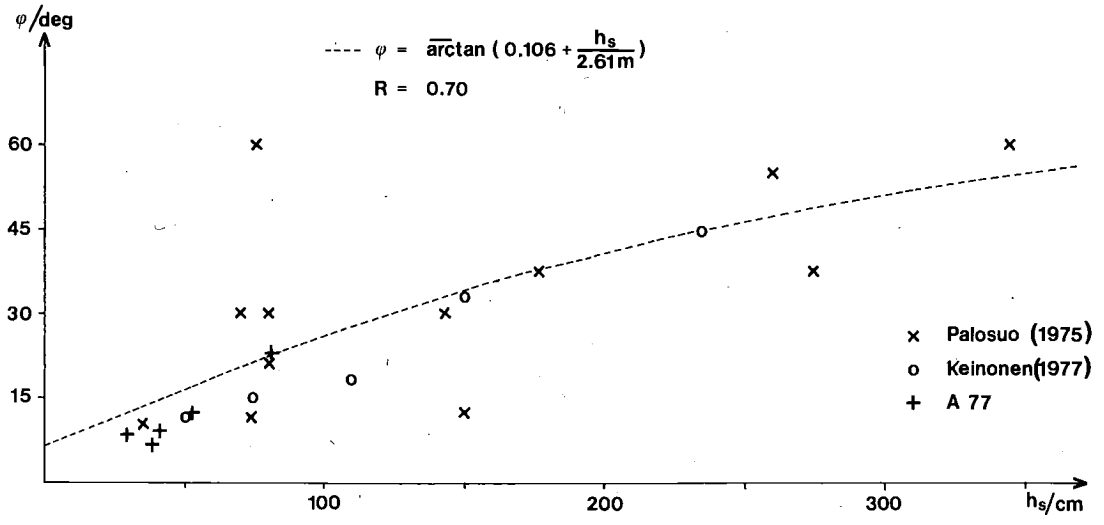

Figure 7. The inclination angle of ridge sails versus sail height. The symbol A77 stands for observations made by the author in March 1977 in the Bothnian Bay.

For small ridges $l_p \approx l_s$, $B \approx 1$ and thus

$$< \frac{h_p}{h_s} > \approx 1 \quad . \tag{2.7}$$

As the ridge size increases, the factor $1-\frac{1}{3}\cdot\frac{l_p}{l_s}$ increases and B decreases.

Empirical comparison between h_p and h_s was once made in the winter 1978/79. One ridge in the northern Bothnian Bay was measured both by levelling and with the profilometer. The results were (in cm):

	I	II
h_p	40	67
h_s	46	75
h_p-h_s	-6	-8

where h_s in the levelling result and I and II refer to the different sides of the ridge. The conclusion is that there is no significant difference between h_p and h_s; the accuracy of the profilometer is $\pm$ 12 cm ($\pm$ 10 cm $\pm$ $10^{-3}\cdot d$ and $d \approx 20$ m) and there is the possibility that the profilometer and levelling lines were not coincident. The formula (2.7) thus holds also for ridges of average size.

On the basis of the foregoing discussion, the working hypotheses that (2.7) holds for all ridges is made. Its validity, especially for large ridges, ought to be checked at some point in the future. A certain amount of support also comes from the fact that the profilometer data on large sail heights agree rather well with the visual image about the ice field during the time when the measurements were made and with what is previously known about Baltic sea ice ridges.

Baltic ice fields generally have snow cover. In further studies it is necessary to know the sail heights above the ice surface and above the water-line in addition to the sail height above the snow cover. Hence level ice thickness and the thickness and density (or at least quality) of snow on ice must be observed.

The actual and measured ridge spacings

Due to slowing down of the ship when penetrating ridges, the measured ridge intervals become larger than the actual intervals, especially when the ridges are close together. No correction for this error is applied in this work and this should be borne in mind when looking at the spatial distributions of ridges. However, statistical decisions have been made ignoring spacings of less than 20 m.

Data analysis

In the Institute of Marine Research in Helsinki the surface profile is plotted on a list by the computer and ridges are manually identified from the list (Fig. 8). The manual work is time-consuming and will be automatized in the future, when operational use of the profilometer gets under way. Examples of methods for automatic ridge pick-up have been given in HIBLER et al. (1972) and WADHAMS (1979).

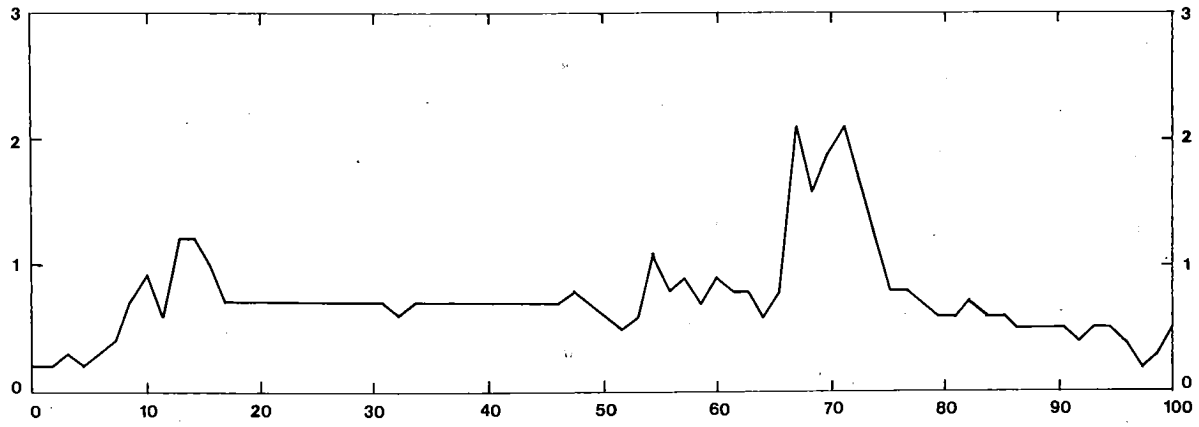

Figure 8. An example of a plotted profile. The numbers in the axis show horizontal and vertical distance (in meters) from an arbitrarily chosen origin.

3. OBSERVED SAIL HEIGHT AND RIDGE SPACING DISTRIBUTIONS

In the winter 1978/79 two series of profile measurements were made: the first (series A) on 1-2 February in the Bothnian Bay and the second (series B) on 1-3 March in the whole Gulf of Bothnia (Fig. 9). The histograms for the observed sail heights and ridge spacings are shown in Figs. 10 and 11 and some standard statistics are given in Table 1.

Table 1. The basic statistics for the profiles: L - total length, h_s - sail height, n - number of ridges with $h_s \geq 30$ cm, μ - ridge density; $\langle \cdot \rangle$ stands for averaging and σ for standard deviation.

	L/km	n	μ/km^{-1}	$\langle h_s \rangle$/cm	σ_{h_s}/cm
A1	12.9	53	4.1	67	50
A2	9.0	88	9.8	51	30
A3	9.2	75	8.2	45	16
A4	9.2	60	6.5	38	6
B1	9.2	48	5.2	47	21
B2	10.4	22	2.1	50	22
B3	6.7	148	22.1	56	29
B4	13.5	45	3.3	51	21
B5	9.8	42	4.3	42	12
B6	7.3	102	14.0	50	26
B7	9.5	45	4.7	47	18

Sail height distribution

The cutoff height h_o must first be specified. Since the accuracy of the profilometer is $\pm$ 12 cm, it is thought that measured height differences less than 30 cm can be due to uneveness of the snow surface and vibration of the ship; hence h_o = 30 cm.

General features in the distributions for $h_s \geq h_o$ are that the mode is at the cutoff height and the density function decreases rapidly with increasing h_s.

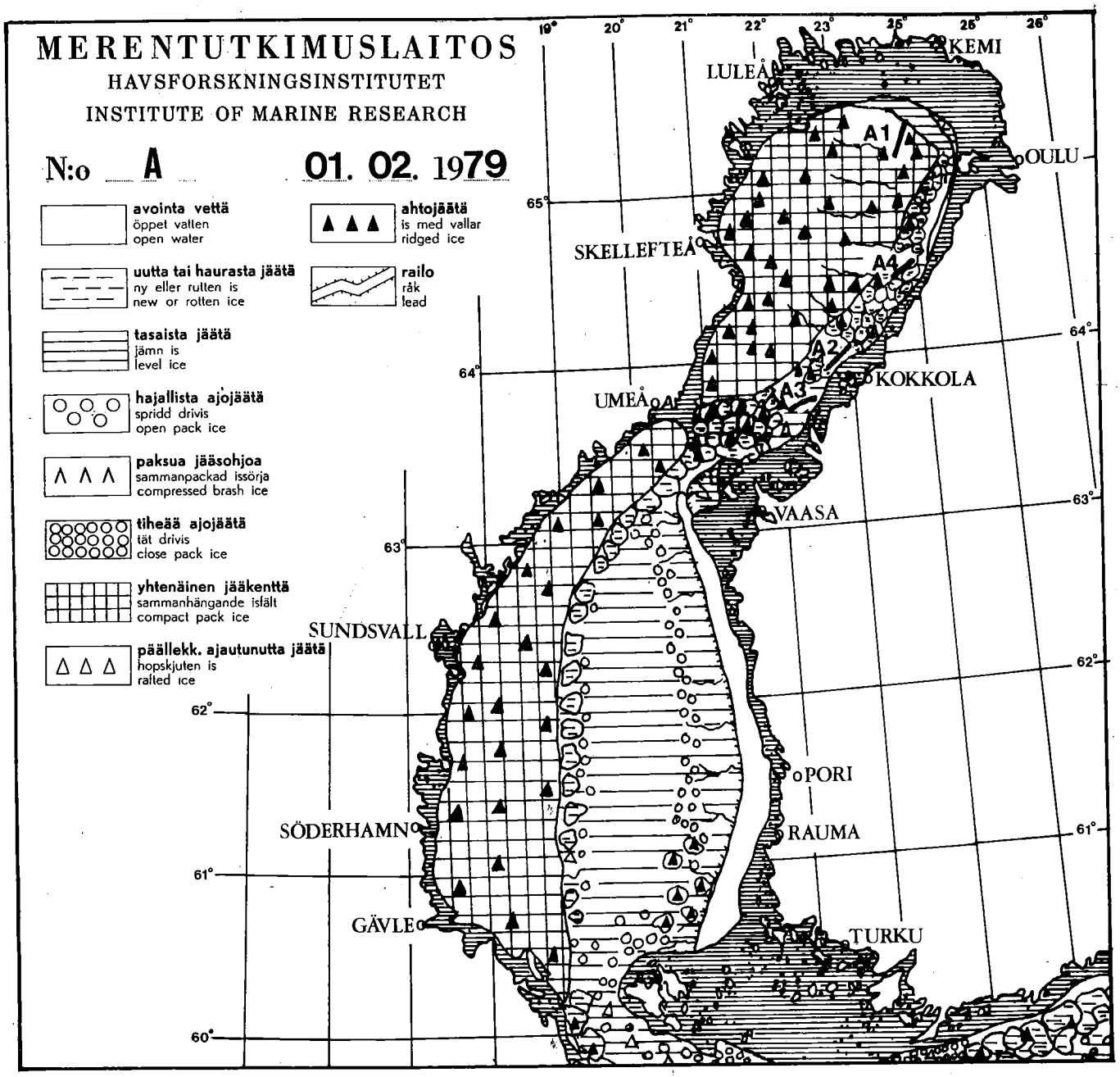

Figure 9a. The profiles obtained during the experiment A on 1-2 February 1979. The length scale of the profiles is the map scale doubled.

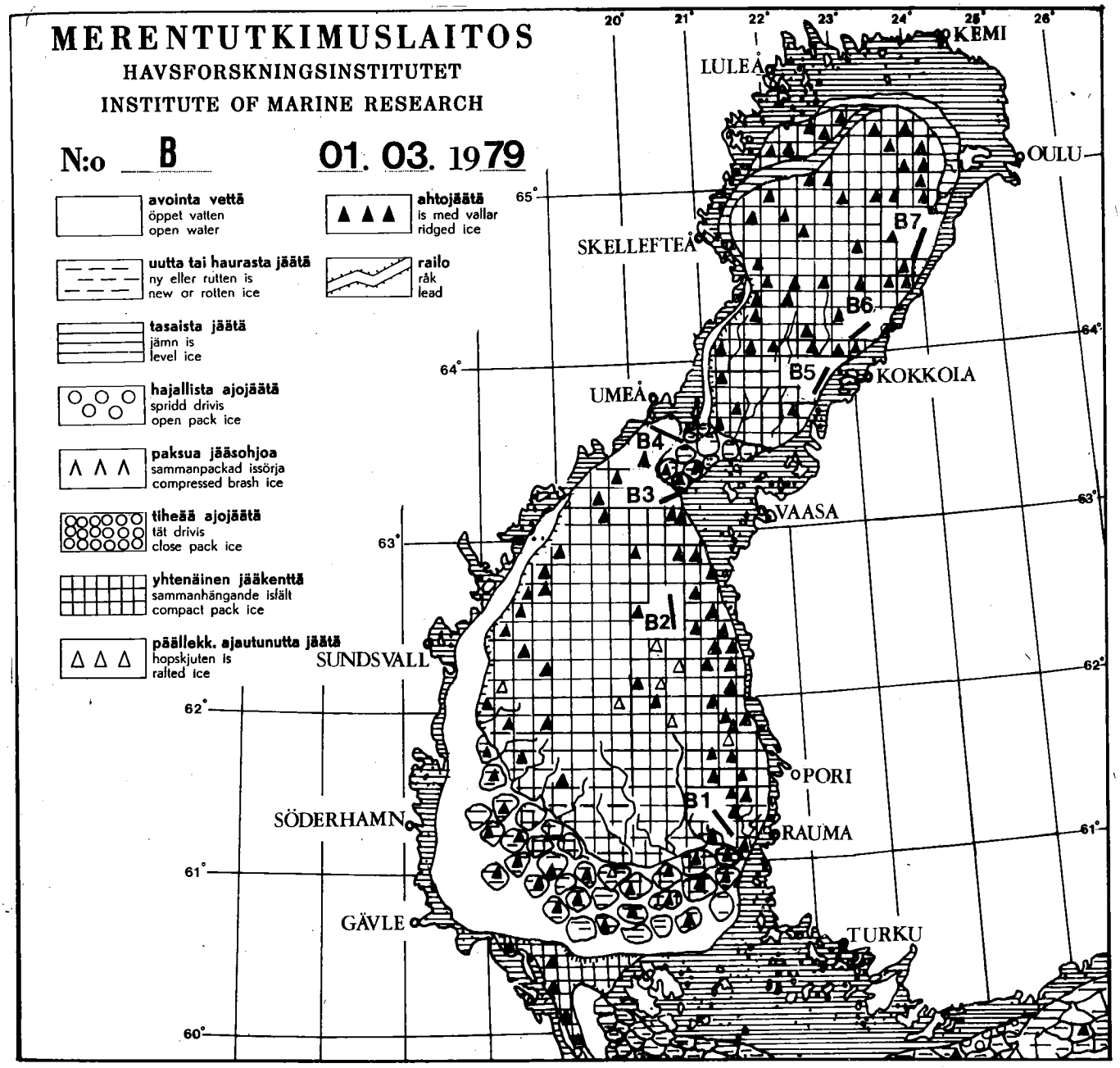

Figure 9b. The profiles obtained during the experiment B on 1-3 March 1979. The length scale of the profiles is the map scale doubled.

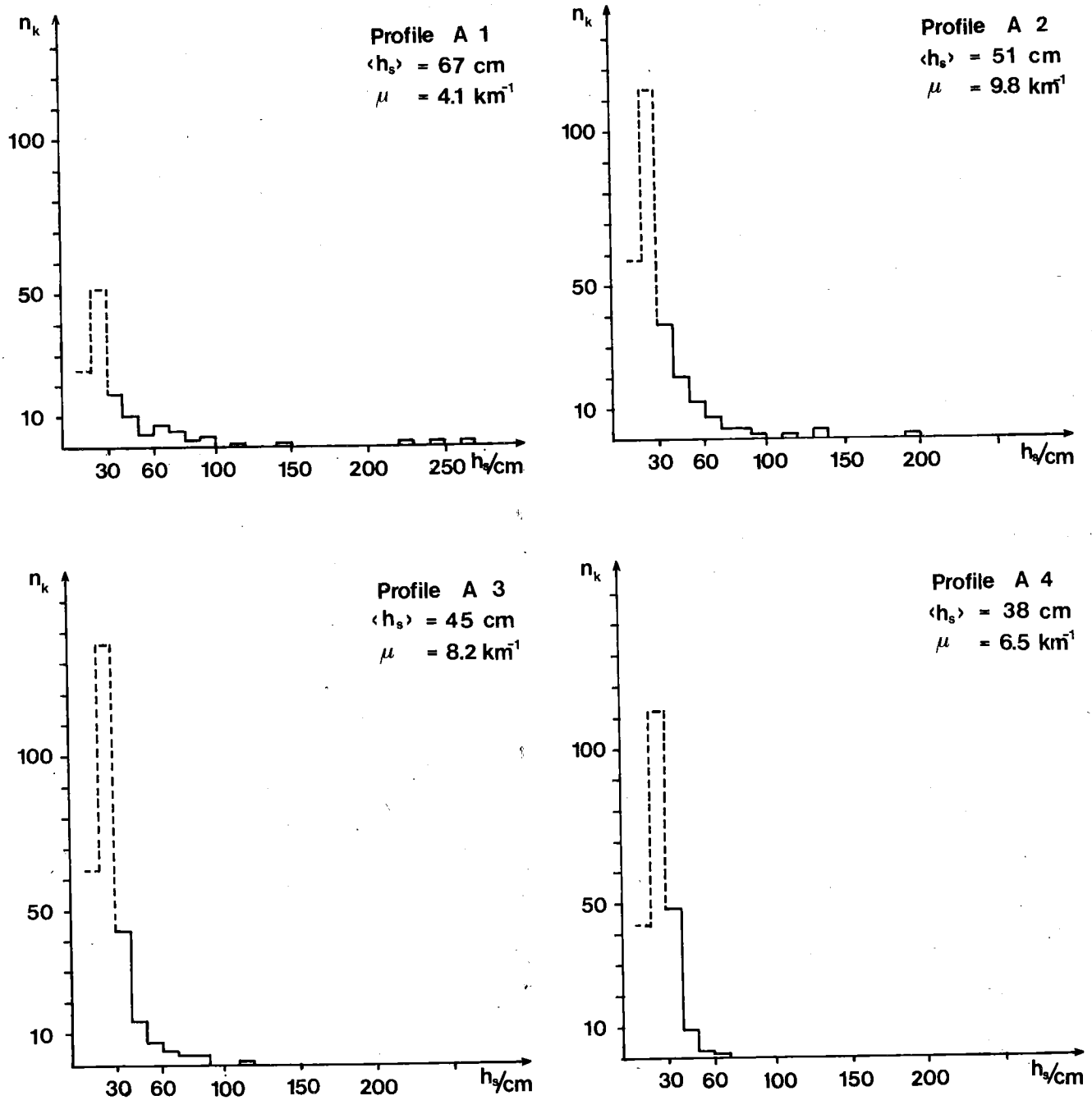

Figure 10a. Distribution of sail heights h_s during the experiment A. Class interval 10 cm and n_k gives the number of cases in each class; cutoff height 30 cm.

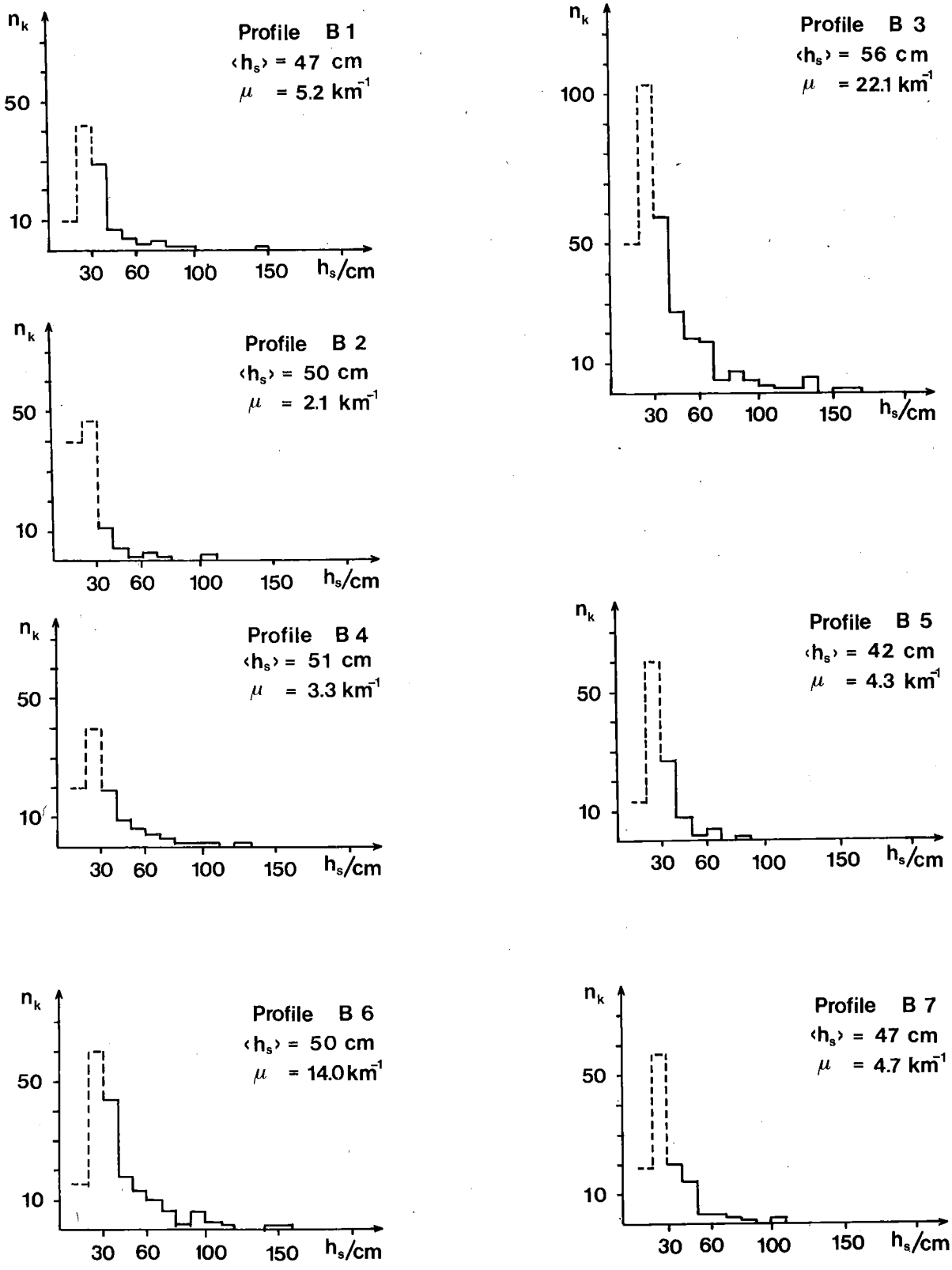

Figure 10b. Distribution of sail heights h_s during the experiment B. Class interval 10 cm and n_k gives the number of cases in each class; cutoff height 30 cm.

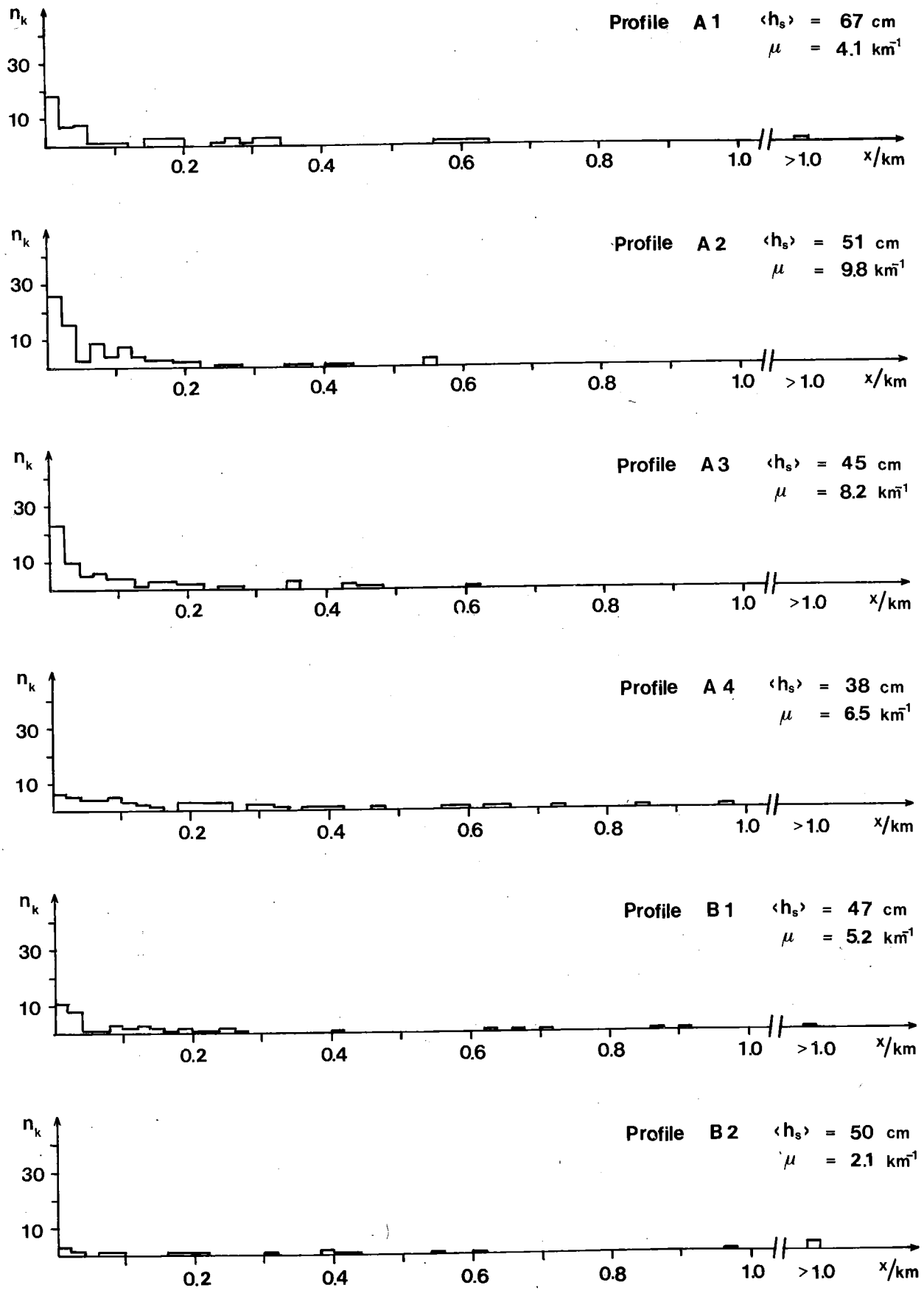

Figure 11, 1st page. For clarifications, see the foot of the next page.

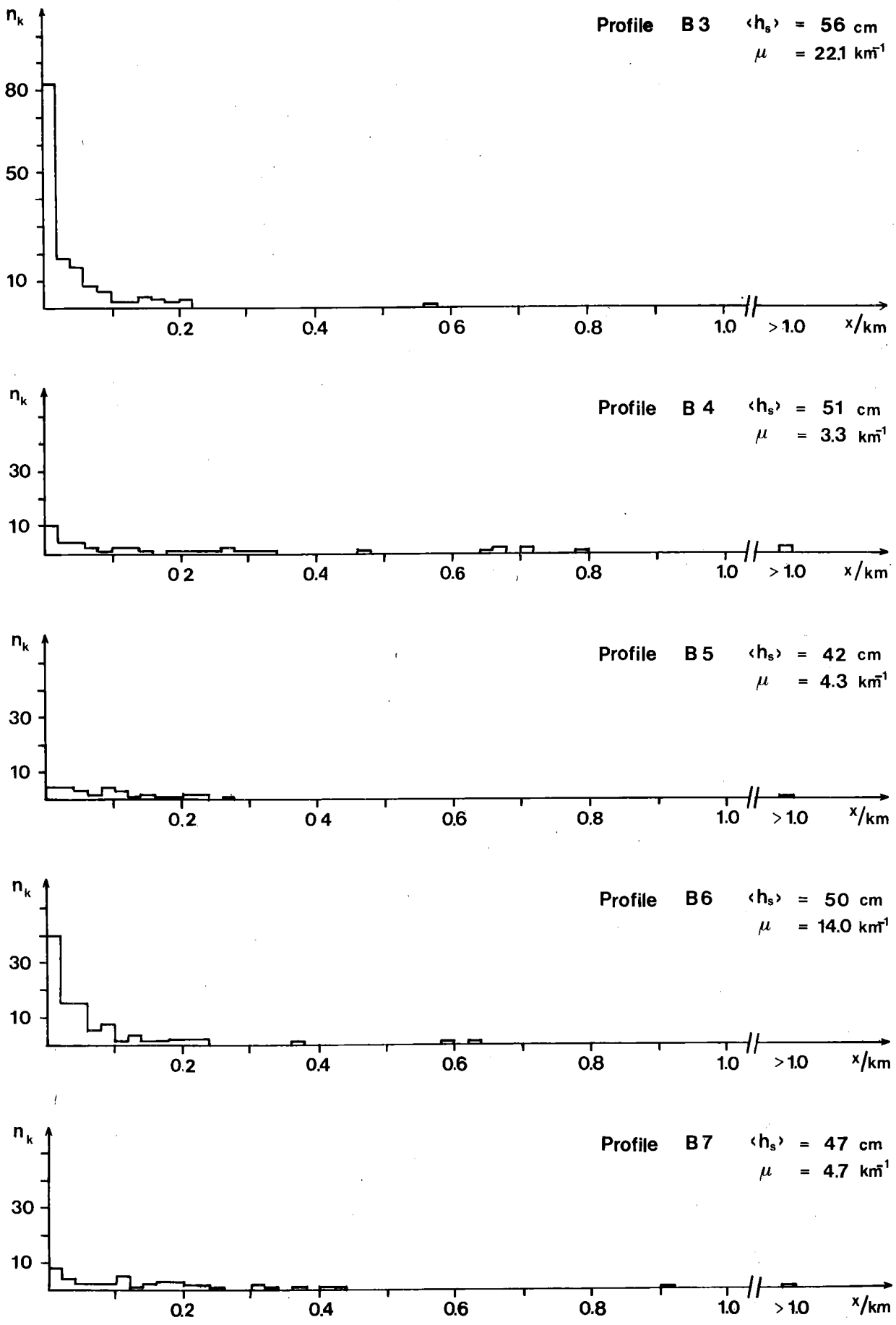

Figure 11, 2nd page. Distribution of ridge spacings during the experiments A and B. Class interval 20 m and n_k gives the number of cases for each class; cutoff height 30 cm.

Using the assumptions of a) geometric similarity of ridge cross-sections and b) equal probability of height arrangements yielding the same net deformation, HIBLER et al. (1972) showed that

$$p(h_s) \propto \exp\left\{ - \lambda' A(h_s) \right\} \quad , \tag{3.1}$$

where $p(\cdot)$ is the probability density function, $A(\cdot)$ cross-sectional area of ridges and λ' a shape parameter. Assuming further that $A(h_s) \propto h_s^2$, Hibler et al. arrived at

$$p(h_s;\ \lambda, h_o) = \frac{1}{\operatorname{erfc}(\sqrt{\lambda}\, h_o)} \cdot 2 \sqrt{\frac{\lambda}{\pi}}\ e^{-\lambda h_s^2}\ S(h_s - h_o),$$

where erfc is the complementary error function and S a step function defined by

$$S(x) = \begin{cases} 1, & \text{if } x \geq 0 \ , \\ 0, & \text{if } x < 0 \ . \end{cases}$$

This distribution, abbreviated below as the HWM-(Hibler, Weeks and Mock) -distribution, has been found to fit well the observations. An even better fit was found by WADHAMS (1979) with the exponential distribution

$$p(h_s;\ \alpha_1, h_o) = \alpha_1 e^{-\alpha_1 (h_s - h_o)} S(h_s - h_o) \ ,$$

which is a special case ($\nu = 1$) of the gamma-distribution family

$$p(h_s;\ \alpha, \nu, h_o) = \frac{\alpha^\nu}{\Gamma(\nu)}\ (h_s - h_o)^{\nu - 1}\ e^{-\alpha (h_s - h_o)} S(h_s - h_o),$$

where

$$\Gamma(\nu) = \int_0^\infty t^{\nu - 1}\ e^{-t}\ dt$$

is the Eulerian gamma-function.

The HWM- and exponential distributions are, h_o being fixed, one-parameter distributions and are completely determined once their mean is known. The gamma-distribution has two parameters and allows independence between mean and variance. This additional degree of freedom can used to advantage in the future, when relating sail height distribution to, e.g., ice thickness distribution and past weather conditions. In the Baltic Sea, development of sail height distributions from the very beginning can be followed every winter.

The estimates for different parametres are shown in Table 2. The parameter λ is obtained from a graph given in HIBLER et al. (1972) and α_1^{-1} is taken as the mean of $h_s - h_o$. The parameters α and ν are obtained from

$$Eh_s = h_o + \nu/\alpha \quad ,$$

$$D^2h_s = \nu/\alpha^2 \quad ,$$

after first estimating the mean Eh_s and variance D^2h_s of h_s in the usual way.

Table 2. The estimated parameters for HWM- (HIBLER et al. 1972), exponential and gamma-distributions for sail heights and χ^2 - goodness-of-fit test (k = degrees of freedom) for the first two distributions. In the column "test" +/- means that the hypotheses is accepted/rejected at 10, 5 and 1 per cent level of significance as read from left to right.

	HWM			exponential			gamma	
	$\lambda^{-\frac{1}{2}}$/cm	χ^2;k	test	α_1^{-1}/cm	χ^2;k	test	α^{-1}/cm	ν
A1	80	7.15;5	+++	37	4.76;5	+++	67	0.55
A2	53	6.29;4	+++	21	1.23;4	+++	43	0.48
A3	41	6.81;2	--+	15	3.14;2	+++	17	0.90
A4	30	5.52;1	--+	8	2.13;1	+++	5	1.56
B1	46	10.75;2	---	17	5.34;2	-++	25	0.64
B2	51	3.71;1	-++	20	2.94;1	-++	23	0.87
B3	64	23.23;6	---	26	8.91;6	+++	33	0.80
B4	54	2.95;3	+++	21	1.60;3	+++	20	1.04
B5	35	2.51;1	+++	12	1.01;1	+++	12	1.04
B6	51	26.37;4	---	20	3.65;4	+++	33	0.61
B7	47	3.70;2	+++	17	2.46;2	+++	17	1.00

It is a striking feature that in all cases the exponential distribution fits the observations better than the HWM-distribution (Table 2). The former always passes the test at the 5 % level. The χ^2-values for the gamma-distribution have not been calculated, because a direct comparison of χ^2-values between one- and two-parameter distributions does not tell us very much. In any event the exponential distribution belongs to the gamma family which therefore cannot be rejected out of hand.

The exponential distribution is the member in the gamma family with $\nu = 1$. In 6 cases out of the total 11 the estimated ν deviates by less than 20 % from unity and the maximum and minimum estimates for ν are 1.56 and 0.48. Remembering that $\sqrt{\nu}$ is equal to the ratio $(Eh_s - h_o)/Dh_s$, it is seen that deviations of ν from 1 are not large. On average, ν tends to be smaller than 1 and this means that the exponential distribution tends to give too small standard deviations relative to the mean.

Distribution of ridge spacings

From the assumption of spatially random occurrence, HIBLER et al. (1972) showed that the distribution of the spacings between adjacent ridges follows the exponential distribution

$$p(x) = \mu e^{-\mu x} S(x) \quad , \tag{3.2}$$

where μ is the ridge density. Testing (3.2) against experimental data by MOCK et al. (1972) gave reasonably good agreement.

The profilometer observations support (3.2) in 7 cases out of 11 at the 5 % level (Table 3). There have been discussions whether the exponential distribution is realistic for small spacings (e.g. LOWRY & WADHAMS 1979). This cannot be pursued here due to the uncertainty of small spacings in the data, as was pointed out in chapter 2, above.

Correlation between ridge density and sail height

It was observed by HIBLER et al. (1972) that ridge density and mean keel depth in different tracks are positively correlated (the correlation coefficient was 0.90). This obviously means

Table 3. χ^2 - goodness-of-fit test of exponential distribution for ridge spacings. In the column "test" +/- means that the hypotheses is accepted/rejected at 10, 5 and 1 per cent level of significance as read from left to right.

	χ^2	k	test		χ^2	k	test
A1	13.75	4	---	B1	8.08	4	-++
A2	3.42	3	+++	B2	0.32	1	+++
A3	5.18	4	+++	B3	11.32	1	---
A4	14.37	4	---	B4	3.11	4	+++
				B5	4.48	4	+++
				B6	8.09	2	--+
				B7	4.01	3	+++

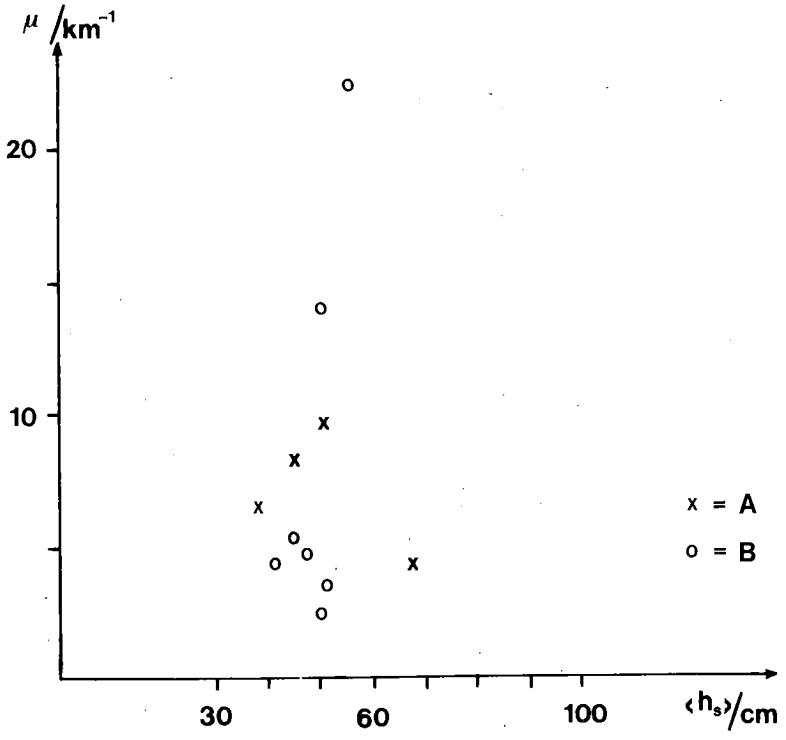

Figure 12. Ridge density versus mean sail height for the profiles of the experiments A and B.

that there is a positive correlation between ridge density and mean sail height. In the Baltic Sea, however, no such correlation is found (Fig. 12).

4. EARLIER OBSERVATIONS IN THE BALTIC SEA

Quantitative observations of statistical features of Baltic ice ridges were begun at the time when the study of large-scale dynamics of sea ice began. Characteristic features of ridging in the Baltic Sea prior to that have been summarized by PALOSUO (1975).

The winter 1976/77

The first empirical distributions of ridge spacings were obtained by LEPPÄRANTA (1979). This data were based on visual counts from a helicopter along two perpendicular tracks in the central Bothnian Bay in March 1977. The track lengths were 10-11 km. The ridge densities in the tracks were 7.0 and 7.9 km^{-1} and the hypotheses of exponential distribution of ridge spacings was accepted for the first and rejected for the second track at 1 % level of signifigance. During that experiment no quantitative information of sail height distributions was obtained.

The winter 1977/78

In the winter 1977/78 the profilometer was used for the first time from an ice-breaker deck. The experiment was made by Palosuo on 23 March in the Bothnian Bay off the coast at Raahe (Fig. 13). The track started at the fast ice edge and was directed westward. It was visually observed that the area had the highest ridge density in the Finnish side of the Bothnian Bay at that time. The results, which have not been published earlier, are shown in Fig. 14.

In the beginning of April 1978 a field experiment concerned with sea ice dynamics near the fast ice edge was carried out.

The research base was situated at the light-house Ulkokalla in the Finnish side of the Bothnian Bay (Fig. 13). On 2 April five air-photo tracks were taken of the area (scale 1:9000). The length of the tracks was 20-25 km. The number of ridges along one line for each track was calculated. The ridge density was close to 7 km^{-1} on four lines and 11.1 on one (Fig. 13). These numbers are in good agreement with the profilometer results obtained ten days earlier, taking into account the dense ridging in the profilometer area.

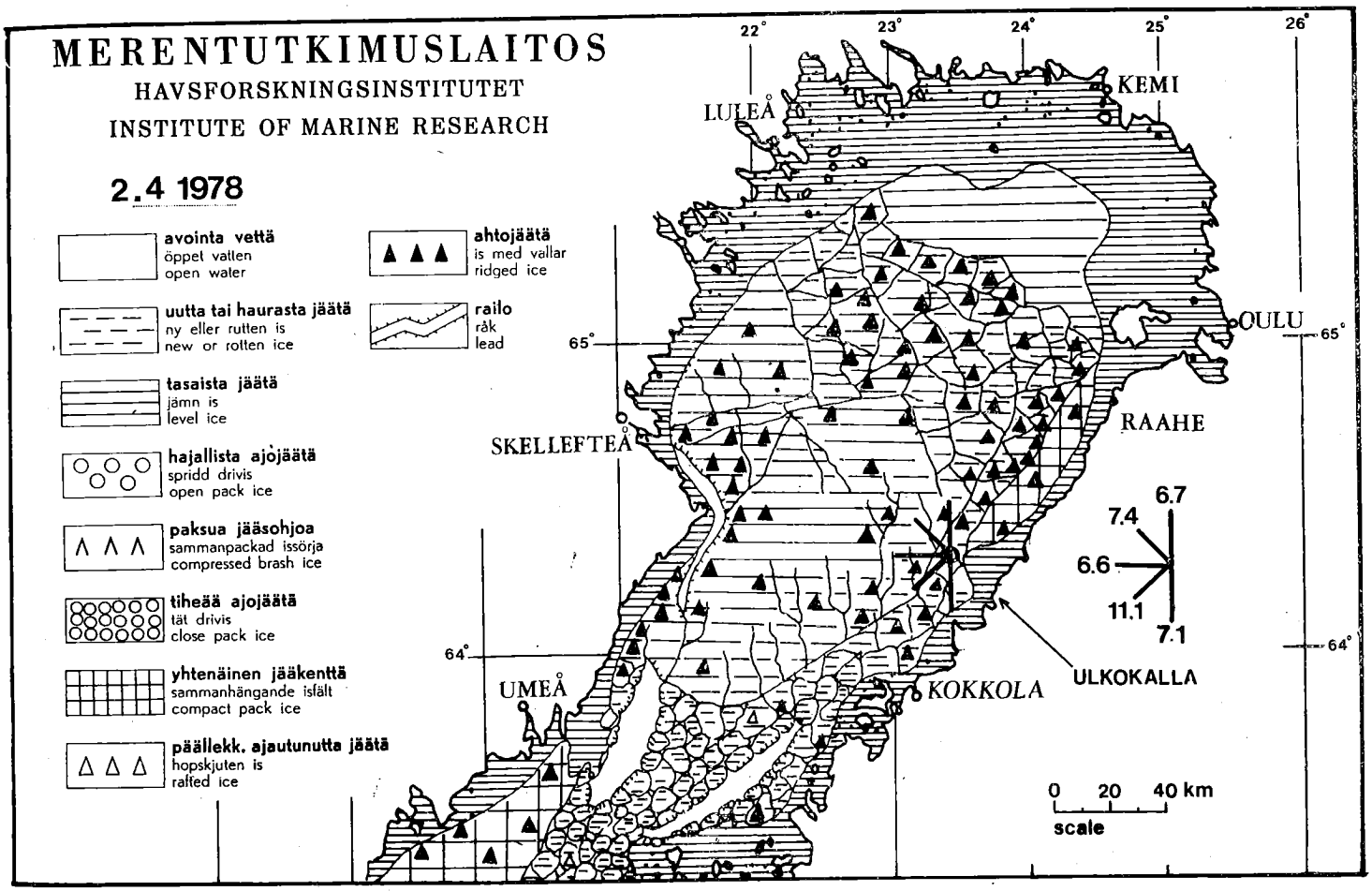

Figure 13. The air-photo tracks taken near Ulkokalla on 2 April 1978. On the right of the map the ridge density in km^{-1} on the tracks is given. The town Raahe on the Finnish side of the Bothnian Bay is shown. Off the coast at Raahe the first run with the profilometer from an ice-breaker deck was carried out by Palosuo on 23 March 1978.

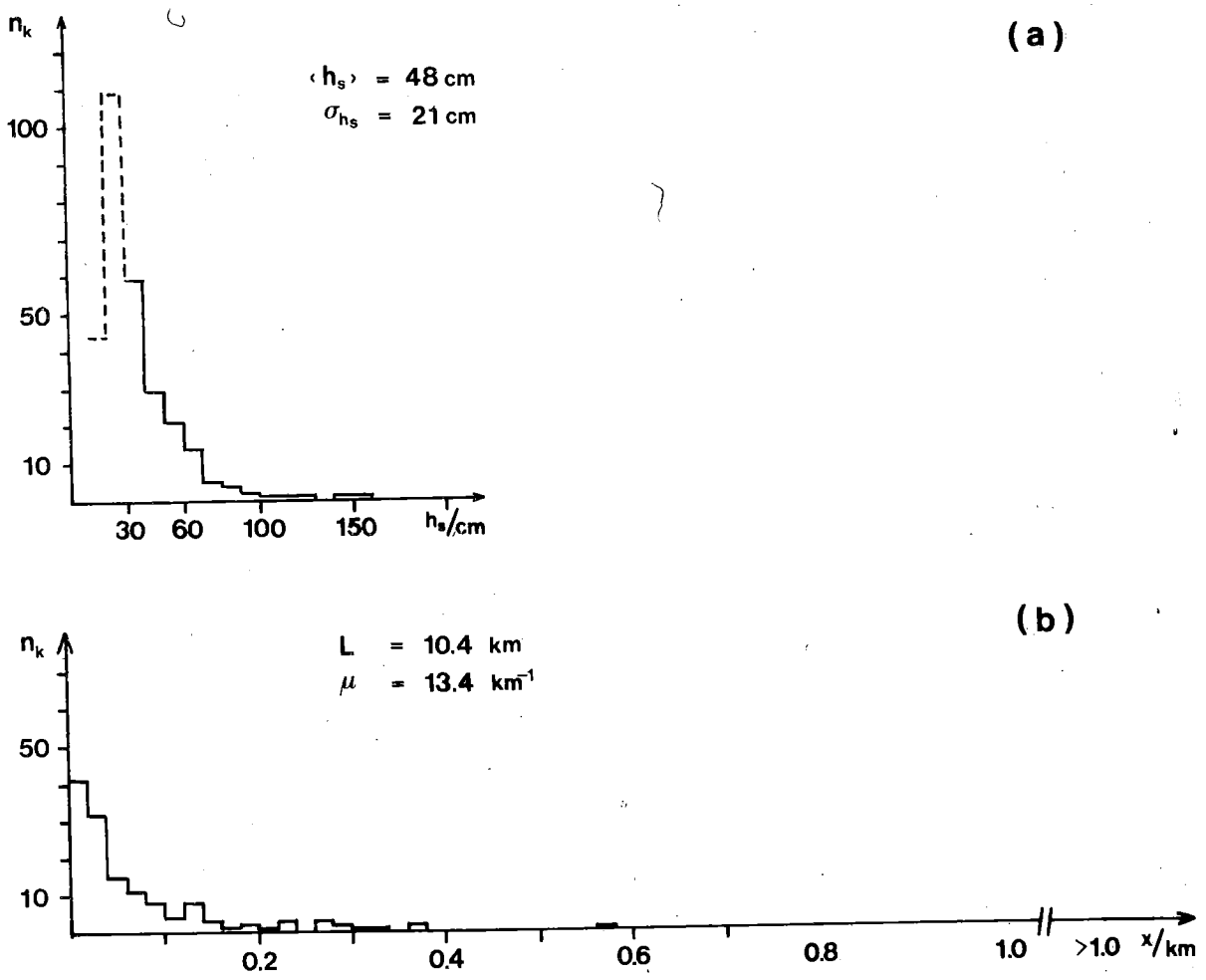

Figure 14. The distributions of (a) sail height and (b) ridge spacing on 23 March 1978 off the coast at Raahe (PALOSUO 1978). The length of the track is L; the cutoff height is 30 cm.

5. DISCUSSION

At the present time data on the spatial characteristics of sea ice ridges are generally obtained along linear tracks: airborne laser-profiling and subsurface sonar profiling studies have been pursued vigorously in the Arctic Ocean during the 70's and now laser-profiling from an ice-breaker deck has been initiated in the Baltic Sea. In such experiments the data are stored on magnetic tapes and hence statistical analysis can be easily and quickly made through automatic data processing.

The statistical features along linear tracks are well described using three parameters: cutoff height, ridge density and mean sail height (or keel depth). They are themselves quite informative. In further analysis the problem is to estimate from these parametres the mass of ridged ice and to describe areal features of ridging. First of all a detailed model for the sail profile is needed.

The model for ridge sails

Two different concepts for the sail height must be used: h_s or h_s' is the maximum elevation of a ridge over the surface of snow or ice, respectively, in the neighbourhood of the ridge (Fig. 15). The former corresponds to the visual image from above and is the sail height measured by the profilometer, while the latter must be used when the mass of ridged ice is studied. Clearly, they are related through

$$h_s' = h_s + H_s \quad ,$$

where H_s is the thickness of snow.

It is assumed that the sail profiles above the snow and ice surfaces are geometrically similar, as indicated in Fig. 15. Then the cross-sectional areas of a ridge above the snow and ice surfaces become

$$A_s = A_s(h_s', \phi) \quad ,$$

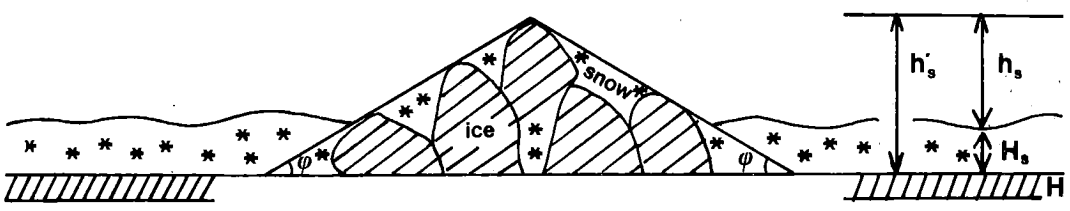

Figure 15. The model for ridge sails.

$$A'_s = A'_s\,(h'_s\,,\,\phi\,)\quad,$$

respectively, and

(4.1) $$A'_s = A_s + D_s\,(h_s\,,\,H_s\,,\,\phi\,)\quad,$$

where D_s is a correction term to the "visual sail profile" due to snow on ice.

A functional form for A'_s is now established starting from (4.1). From simple trigonometry it is seen that

(4.2.a) $$A_s = h_s^2 \cot\phi\quad,$$

(4.2.b) $$D_s = H_s\,(H_s + 2\,h_s)\cot\phi\quad.$$

The profilometer measurements do not give a usable value for ϕ. For Baltic ice ridges it seems that h_s and ϕ are not independent but are positively correlated (Fig. 7). Through linear regression the parameteres in the equation

(4.3) $$\tan\phi = a + bh_s$$

have been estimated. The correlation coefficient for (4.3) was 0.70 and the parameters with their standard deviations were

$$a = 0.106 \pm 0.073\quad,$$
$$b = 0.383\ m^{-1} \pm 0.084\ m^{-1}\quad.$$

Then, from (4.2) and (4.3)

(4.4.a) $$A_s = \frac{h_s^2}{a+bh_s}\quad,$$

(4.4.b) $$D_s = H_s \cdot \frac{2h_s + H_s}{a+bh_s}\quad,$$

and finally

$$A'_s = \frac{h_s^2}{a+bh_s} + H_s \cdot \frac{2h_s + H_s}{a+bh_s} \quad . \tag{4.5}$$

From consideration of equation (4.4a) two special cases arise: (i) $a = 0$ gives $A_s \propto h_s$, which means that the sail width is a constant ($= b^{-1}$) for all sail heights, and (ii) $b = 0$ gives the commonly used assumption $A_s \propto h_s^2$ (e.g. HIBLER et al. 1972), which means that the angle ϕ is a constant ($= \overline{\text{arc}}\ \tan a$). Reality lies somewhere "between" (i) and (ii), but it is noted that the estimated a is not significantly different from zero, while b is. This poor agreement of $A_s \propto h_s^2$ with the data may be one reason why the fit of the HWM-distribution was worse than that of the exponential (chapter three, above).

Ridge sails consist of ice blocks and snow (Fig. 15). The important inter-structural parameters of sails are the densities and porosities of ice blocks and snow, while in case of ridge keels the density and porosity of ice blocks are important. The values and notations for these parameters used here are given in Table 4.

The area A'_s can be written

$$A'_s = A'_{s,i} + A'_{s,s} \quad , \tag{4.6}$$

where

$$A'_{s,i} = (1-\nu_{s,i})\ A'_s \quad , \tag{4.7.a}$$

$$A'_{s,s} = (1-\nu_{s,s})\ A'_s \quad , \tag{4.7b}$$

are the cross-sectional areas of ice blocks and snow, respectively, in the sail. Finally, the expression for A'_s becomes, from (4.1), (4,6) and (4.7),

$$A'_s = (1-\nu_{s,i})\,(A_s + D_s) + (1-\nu_{s,s})\,(A_s + D_s) \quad , \tag{4.8}$$

and A_s and D_s are functions of h_s and H_s only, given in (4.5).

Table 4. Inter-structural ridge parameters and the values used for them.

Parameter	Notation	Value	Reference
Density of			
sail ice	$\rho_{s,i}$	0.87 Mg m^{-3}	KEINONEN (1977)
sail snow	$\rho_{s,s}$	0.37 Mg m^{-3}	KEINONEN (1977)
keel ice	ρ_k	0.91 Mg m^{-3}	assumption
Porosity of			
sail ice	$\nu_{s,i}$	0.4	KEINONEN (1977)
sail snow	$\nu_{s,s}$	0.6	KEINONEN (1977)
keel ice	ν_k	$= \nu_{s,i}$	assumption

The cross-sectional profile of ridges

The mass of the sail per unit width is obtained from (4.8) through adding the densities:

$$m_s = \rho_{s,i}(1-\nu_{s,i})A'_s + \rho_{s,s}(1-\nu_{s,s})A'_s \quad .$$

The isostatic principle states that

$$m_s + \rho_k(1-\nu_k)A_k = \rho_w(1-\nu_k)A_k \quad ,$$

where A_k is the cross-sectional area of the ridge keel and ρ_w the density of water (= 1.005 Mgm^{-3}), and thus

$$A_k = \left\{ \frac{1-\nu_{s,i}}{1-\nu_k} \cdot \frac{\rho_{s,i}}{\rho_w - \rho_k} + \frac{1-\nu_{s,s}}{1-\nu_k} \cdot \frac{\rho_{s,s}}{\rho_w - \rho_k} \right\} \cdot A'_s \quad . \tag{4.9}$$

Then the total area of ice blocks in the ridge $A_{r,i}$ becomes, from (4.7.a) and (4.9),

$$A_{r,i} = A'_{s,i} + A_k = \kappa \cdot A'_s \quad ,$$

where $\kappa \approx 13$ (from Table 4).

Since in a ridge most of the ice mass per unit width, $m_{r,i}$, is in the keel, we approximate $m_{r,i} \approx \rho_k (1 - \nu_k) A_{r,i}$. The total mass of the ridge is snow mass + ice mass. The ratio of these two is

$$\frac{m_{r,s}}{m_{r,i}} = \frac{\rho_{s,s}(1 - \nu_{s,s})}{\rho_k (1 - \nu_k)\kappa} \sim 1 \ \% \quad .$$

Thus the relative mass of snow in ridges is small as compared with a typical value of ~ 10 % for level ice.

The amount of ridged ice

It is often convenient to express the amount of ridged ice in terms of equivalent ice thickness H_e. That is, for a given line or area, to express what thickness of continuous ice sheet would contain an ice mass equal to the mass of ridged ice in the line or area under consideration.

The equivalent ice thickness along a linear track is

(4.10) $$H_e = \mu \kappa < A'_s > \quad ,$$

where μ is the ridge density along the track. Assuming that h_s follows the exponential distribution with parameters α_1 and h_o, averaging of (4.4) over $h_s \geq h_o$ gives (a and b>0)

(4.11.a) $$<A_s> = \frac{1}{b} \left\{ <h_s> - \frac{a}{b} + \left(\frac{a}{b}\right)^2 \alpha_1 e^{\alpha_{1*}} E_1(\alpha_{1*}) \right\} \quad ,$$

$$(4.11.b) \qquad \langle D_s \rangle = \frac{H_s}{b} \left\{ 2 + \alpha_1 (H_s - 2\frac{a}{b}) e^{\alpha_{1*}} E_1 (\alpha_{1*}) \right\} ,$$

where

$$\alpha_{1*} = (\frac{a}{b} + h_o) \alpha_1 ,$$

and

$$E_1(y) = \int_y^\infty \frac{1}{t} e^{-t} dt$$

is the exponential integral. And, finally

$$\langle A_s' \rangle = \langle A_s \rangle + \langle D_s \rangle .$$

The expression for $\langle A_s' \rangle$ is rather cumbersome involving, as it does, exponential integrals which must be numerically evaluated (tabulated in ABRAMOWITZ & STEGUN 1972). With the values estimated here for a and b and with typical Baltic sail height distributions, $\langle A_s \rangle$ and $\langle D_s \rangle$ obtained simply through using $\langle h_s \rangle$ in (4.4) do not differ significantly from those obtained from (4.11). Further more, it should be noted that the relative part of $\langle D_s \rangle$ in $\langle A_s' \rangle$ was 10-30 % in the observations presented here.

In deriving (4.11) it was assumed that a, b >0. With the classical assumption of b = 0 (i.e. ϕ = constant = $\overline{\text{arc}}$ tan a) things become somewhat simpler. Thus,

$$\langle A_s \rangle = \frac{1}{a} \left\{ \langle h_s \rangle^2 + (\langle h_s \rangle - h_o)^2 \right\} ,$$

$$\langle D_s \rangle = \frac{1}{a} \left\{ H_s^2 + 2 H_s \langle h_s \rangle \right\} ,$$

where the term $(\langle h_s \rangle - h_o)^2$ arises from integration due to non-linearity of $A_s = A_s (h_s)$.

In estimating the equivalent ice thickness in an area, H_e^* , from the information for a linear track, directional isotropy in ridging is assumed. Then, according to MOCK et al. (1972)

(4.12.a) $$H_e^* = \frac{\pi}{2} H_e = \frac{\pi}{2} \mu\kappa \cdot \langle A_s' \rangle \quad .$$

The validity of the hypotheses on directional isotropy is not well established for Baltic ice conditions. It may be poor near the coast. The data based on visual observations show no significant difference in ridge density along two perpendicular tracks in the central Bothnian Bay (LEPPÄRANTA 1979).

The estimated equivalent ice thickness from the profilometer data vary between 4 and 62 cm (Table 5). In one case (profile B3) it was more than the thickness of level ice. For comparison, values for equivalent ice thickness based on earlier formulas of the type

(4.12.b) $$H_e^{**} = \kappa' \cdot \mu \langle h_s' \rangle^2$$

are shown. The coefficient κ' was taken as $\kappa' = 51$ from LEPPÄRANTA (1979). HIBLER et al. (1974) give $\kappa' = 10\pi$ for Arctic ice conditions.

Table 5. The amount of ridging observed in the experiments A and B: H - level ice thickness, H_s - snow thickness, H_e^* - equivalent ice thickness of ridges estimated from (4.12.a), H_e^{**} - equivalent ice thickness of ridges estimated from (4.12.b), ν - the ridging intensity parameter of HIBLER et al. (1974), μ - ridge density, and h_s - sail height.

	H	H_s	H_e^*	H_e^*/H	H_e^{**}	ν	$10^{-3}\mu\langle h_s \rangle$
	cm	cm	cm		cm	m^2/km	
A1	50	10	13.8	0.28	12.3	2.64	2.75
A2	40	5	21.0	0.53	15.7	2.75	4.96
A3	35	5	15.4	0.44	10.5	1.34	3.67
A4	35	5	9.8	0.28	6.1	0.59	2.46
B1	30	5	9.2	0.31	7.2	1.12	2.43
B2	30	5	4.4	0.15	3.2	0.54	1.06
B3	35	10	61.8	1.77	49.1	9.05	12.35
B4	40	10	8.4	0.21	6.3	0.97	1.70
B5	55	10	8.9	0.16	5.9	0.53	1.80
B6	55	10	34.6	0.63	25.7	3.59	7.01
B7	55	10	9.6	0.17	7.8	1.04	2.25

Descriptions for ridged ice mass different from the concept of equivalent ice thickness exist and the values estimated for two of them from the profilometer data are given in Table 5. HIBLER et al. (1974) defined a ridging intensity parameter ν through $\nu = \mu \lambda^{-1}$, where λ is the shape parameter of the HWM-distribution. The weak point of ν is that the parameter is tied to a particular kind of distribution, as pointed out by TUCKER et al. (1979).

ARYA (1973) came up with the dimensionless quantity $\mu\langle h_s \rangle$, which is directly proportional to the sum of the vertical projections of sail height per unit length and can be used to parametrize the form drag due to ridge sails. From BANKE & SMITH (1975) it is estimated that the form drag coefficient for Baltic ice ridges should be $\sim 0.1\ \mu\langle h_s \rangle$ and thus it can be significant compared with the drag-coefficient of tangential shear ($\approx 1.5 \cdot 10^{-3}$) (Table 5).

Soviet scientists have used a ridging number which is determined from the relative area of ridged ice (ZUBOV 1945). This, however, is very difficult to define. In relating the ridging number to the equivalent ice thickness a wide scatter is found in the work of different authors (Fig. 16, GUDKOVIC & ROMANOV 1976).

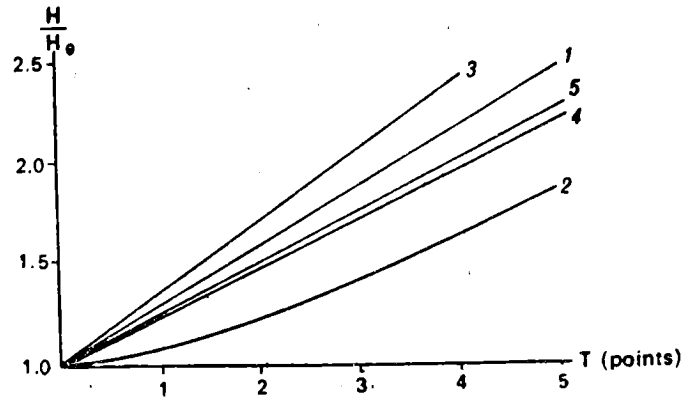

1—according to P.A. Gordienko; 2—A.A. Kirillov; 3—A.Ja. Buzuev and N.P. Sesterikov (the value of melting $\Delta H = 70$ cm); 4—the same for $\Delta H = 0$; 5—according to G.N. Sergeev.

Figure 16. Total ice mass thickness versus the point of hummocking T (GUDKOVIC & ROMANOV 1976): H_θ is the level ice thickness and $H = H_\theta + H_e^*$, where H_e^* is the equivalent thickness of ridged ice.

The density of large ridges

It is quite important to know the density of the large ridges which are a severe problem to winter navigation. Let us denote by $\mu(h_*)$ the density of ridges with $h_s \geq h_* \geq h_o$, where h_o is the cutoff height, and let $P(\cdot)$ stand for probability. It is easily seen that

$$\mu(h_*) = \mu(h_o) P(h_s \geq h_*) \quad . \tag{4.13}$$

In the case of the exponential distribution with parameters and h_o (4.13) becomes

$$\mu(h_*) = \mu(h_o)\, e^{-\alpha_1 (h_* - h_o)} \quad . \tag{4.14}$$

For example, if it is desired to know the maximum ridge height occurring on average once in, say, one kilometer, the solution is directly obtained from (4.14) with given α_1, h_o and $\mu(h_o)$ and with $\mu(h_*) = 1\ \mathrm{km}^{-1}$.

It should be mentioned here that it follows from the basic properties of the exponential distribution that $\mu(h_*)$ is independent of the choice of the cutoff height. That is, even if the cutoff height is chosen incorrectly, the density of large ridges can be correctly estimated, provided that the hypotheses of the exponential distribution is valid. This will be discussed in detail below.

The exponential distribution tends to underestimate the density of large ridges (Table 6). The explanation is that while the exponential distribution implies equality between $\langle h_s \rangle - h_o$ and standard deviation σ, in reality σ tends to be larger than $\langle h_s \rangle - h_o$. This was seen already in the tendency of ν to be less than unity in the gamma-distribution generalization of the exponential distribution (Table 2). In the case of the HWM-distribution, the underestimation of the density of large ridges is even greater than in the exponential case (Table 6).

The gamma-distribution parameter ν could be used to indicate the degree of variability of sail heights. When ridges are formed from a level ice field with uniform thickness during the first storm, the resulting gamma-distribution probably has $\nu > 1$, but when the variance of ice thickness increases and ridges are formed during subsequent storms, ν decreases. The present data suggest that ν drops below 1 quite soon. One notes that, when $\nu \leq 1$, the mode of the distribution is at the cutoff height. This fact is supported by most studies.

Table 6. The density of large ridges in the experiments A and B. The probability of occurrence of ridges with sail height $\geq h_{*p}$ is p, which has been chosen so that the tail class $[h_{*p}, \infty)$ has at least 5 % probability (differences in p-values are due to the finite class interval of 10 cm), and n_p is the number of ridges in $[h_{*p}, \infty)$. Predictions based on exponential and HWM-distributions are shown.

	observed			predicted h_{*p}/cm	
	p/%	n_p	h_{*p}/cm	exp	HWM
A1	5.7	3	220	136	120
A2	5.7	5	110	89	84
A3	5.4	4	80	74	69
A4	5.0	3	50	53	56
B1	6.3	3	80	76	75
B2	9.1	2	80	78	75
B3	5.4	8	130	106	100
B4	6.7	3	90	87	83
B5	14.3	5	60	53	53
B6	10.8	11	100	75	72
B7	6.8	3	80	77	74

Sensitivity of results to the cutoff height

The choice of the cutoff height is rather subjective and the main reason for the choice of h_o = 30 cm in this work was to prevent snow-drifts and disturbances due to vibration of the ship from being registrated as ice ridges. However, if the sail heights really do obey the exponential distribution, the parameter α_1 is estimated correctly, whatever cutoff height is chosen.

Assume that in reality h_s follows the exponential distribution. The probability density is then

$$p(h_s;\ \alpha_1,\ h_c) = \alpha_1 e^{-\alpha_1(h_s-h_c)} S(h_s-h_c),$$

where h_c is the real but unknown cutoff height such that $0 \leq h_c \leq h_o$. Then the conditional distribution of $h_s \mid h_s \geq h_o$ is again exponential and

$$p(h_s;\ \alpha_1, h_c \mid h_s \geq h_o) = \alpha_1 e^{-\alpha_1(h_s-h_o)} S(h_s-h_o), \tag{4.14}$$

i.e. the estimated α_1 from $h_s \geq h_o$ is the true value. But, of course, the estimated μ and H_e are not the real values. Similarly to the derivation of equation (4.14), it is seen that

$$\mu(h_o) = \mu(h_c) e^{-\alpha_1(h_o-h_c)} . \tag{4.16}$$

When $\alpha_1^{-1} < h_o - h_c$, the estimated ridge density is less than 1/e times the true value. Hence it is important to give both the estimated μ and its argument, i.e. h_o. It should be noted that the densities obtained from the profilometer data with h_o = 30 cm are comparable to the densities based on visual counts and air photos in the Bothnian Bay (see chapter three).

Using the equations (4.14) and (4.16) the density of large ridges with $h_s \geq h_*$ becomes

$$\mu(h_*) = \mu(h_c) e^{-\alpha_1(h_*-h_c)} . \tag{4.17}$$

Since it was shown with (4.15) that the estimate of α_1 does not depend on h_o, it is concluded from (4.17) that also the value of $\mu(h_*)$ in (4.14) is independent of h_o.

Due to the invariance property of α_1, the error in mean sail height due to the choice of the cutoff height is simply $h_o - h_c$. When estimating the mass of ridged ice, the errors in ridge

density and mean sail height tend to balance each other. However, when $\alpha_1^{-1} < h_o - h_c$, i.e. the mean sail height is relatively close to the chosen cutoff height, the estimated H_e can be less than half the true value.

Naturally, there are other sources of error in ice mass estimation than the choice of the cutoff height. Perhaps the most uncertain point at present is the imperfect information on sail and keel porosity. Errors also arise from the estimation of snow thickness and from the variability of sail profile geometry.

Representative sail height

It is still open to discussion exactly what kind of sail height would be a good representative one. The mean sail height used here and in earlier works is a clearly defined quantity, but it does not necessarily agree well with what the ice ridges actually look like from ships. The case is analogous to ocean waves, for which average wave height is not used to express a representative wave height. Another point is that it is not so much average sized ridges, but large ones, which are the problem in winter navigation.

It is proposed here that in future work two kind of representative sail heights should be studied. First, the sail height corresponding to a ridge having the average cross-sectional area and, secondly, the height corresponding to a ridge having the average potential energy. These two types of definition which depend on the higher order terms of h_s rather than the first order, linear term, would be larger than $\langle h_s \rangle$ and the effect of the choice of the cutoff height would then be smaller than on $\langle h_s \rangle$.

CONCLUSIONS

Spatial distributions of ridge sail heights and ridge spacings in the Gulf of Bothnia have been studied. Observations were made during two experiments in February and March 1979 using a laser-profilometer mounted on the deck of the ice-breaker Urho. The following conclusions can be drawn from the results:

1. Use of the laser-profilometer from an ice-breaker deck is a reliable and economic way to make observations of ridges.
2. Three sources of error are present, when measuring sail heights: (i) inclination of the laser-beam with respect to the vertical, (ii) the measured value is an average over a finite interval and not the maximum elevation of the ridge sail, and (iii) the buoyancy of ridges lifts the ship. Errors (i) and (ii) have been treated theoretically and on the basis of experience it was concluded empirically that errors (i)-(iii) cancel out one another.
3. Two sources of error are present, when measuring ridge spacings: (i) the choice of cutoff height, and (ii) the fact that the ice-breaker slows down when going throught a ridge, due to the resistance of the ridge. The latter error was not eliminated from the data, causing thus a degree unreliability in the high-frequency band of the spatial spectrum. The error (i) implies that the observed ridge spacings are in reality the spacings of ridges higher than the cutoff height of 30 cm.
4. The observed histograms of the sail heights and ridge spacings have been presented (Figs. 10-11). Average sail height varied between 38 and 67 cm and ridge density between 2.1 and 22.1 km^{-1}. The exponential distribution for sail heights and ridge spacings was accepted at the 5 % level of significance in 11 and 7 cases, respectively, out of the total 11. The distribution for sail heights derived theoretically by HIBLER et al. (1972) was accepted at the 5 % level of significance in 5 cases. There was no correlation between sail height and ridge density.

5. For further analysis of the data a model for ridge sails has been presented. It is stressed that the part of the sail at lower elevation than the snow surface is not recognized in surface topography measurements and must be taken into account through estimating the thickness of the snow cover. In the Baltic Sea, the inclination and height of sails were shown to be positively correlated and this was taken into account when estimating the average cross-sectional area of sails.
6. An equation for equivalent ice thickness of ridged ice has been derived (eq. 4.12.a). The mass of ridged ice was typically of the order of several tenths of the mass of level ice.
7. The exponential distribution usually underestimated the density of large ridges. It was proposed that a generalization using the gamma-distribution could give better results, since it allows independence between average and variance.
8. The sensitivity of the results to the choice of the cutoff height has been studied. It has been shown that the error in mean sail height is equal to the error in cutoff height and that the choice may strongly affect the ridge density, but causes no error in the estimation of the density of large ridges.
9. It is proposed that the sail height corresponding to a ridge having an average cross-sectional area or average potential energy might be a good representative sail height worthy of further study.

ACKNOWLEDGEMENTS

This research has been carried out at the Institute of Marine Research in Finland. I am extremely grateful to Professor Erkki Palosuo for his ideas for instrumentation and for numerous valuable discussions during the processing of the data. I want to express my sincerest thanks to Tom Artela, the Captain of the ice-breaker Urho, for his hospitality and interest in this

research project. The work has been financially supported by the Board of Navigation, which is gratefully acknowledged.

REFERENCES

Abramowitz, M. & I.S. Stegun 1972: Handbook of mathematical functions. - Dover Publications, Inc., 1046 p. New York.

Arya, S.P.S. 1973: Contribution of form drag on pressure ridges to the air stress on Arctic ice. - J. Geophys. Res. 78(30): 7092-99.

Banke, E.G. & S.D. Smith 1975: Measurement of form drag on ice ridges. - AIDJEX Bull. 28:21-27.

Gudkovic, Z.M. & M.A. Romanov 1976: Method for calculation the distribution of ice thickness in the Arctic seas during the winter period. - In: Krutskih, B.A., Z.M. Gudkovic & A.L. Sokolov (ed.): Ice Forecasting Techniques for the Arctic Seas, pp. 1-48. New Delhi (translated from Russian).

Hibler, W.D., III, W.F. Weeks & S.J. Mock 1972: Statistical aspects of sea ice ridge distributions. - J. Geophys. Res. 77(30):5954-70.

- " - , S.J. Mock & W.B. Tucker III 1974: Classification and variation of sea ice ridging in the Western Arctic Basin. - J. Geophys. Res. 79(18):2735-43.

Keinonen, A. 1977: Measurements of physical characteristics of ridges on April 14 and 15, 1977. - Winter Navigation Research Board, Res. Rep. No 22, 20 p. Helsinki.

Ketchum, R.D., Jr. 1971: Airborne laser profiling of the Arctic pack ice. - Remote Sensing of the Environment 2:41-52.

Leppäranta, M. 1977: Pohjanlahden jääennustusmalli. [Model for ice forecast in the Gulf of Bothnia.] - In: Helminen, J. (ed.): Geofysiikan päivät Helsingissä 10.-11.3.1977, pp. 291-300. Geophysical Society of Finland, Helsinki.

- " - 1979: On the dynamics of ice cover in the Bothnian Bay. - Ice, Ships and Winter Navigation. Proceedings of the Symposium in Oulu University 1977-12-16...17 in connection with the 100 Year Celebration of Finnish Winter Navigation, pp. 132-52. Board of Navigation, Helsinki.

- " - 1980: Ice drift model for the Baltic Sea. - Paper presented at the XII Meeting of Baltic Oceanographers, 14-19 April 1980, Leningrad, 32 p. (mimeogr.).

Lowry, R.T. & P. Wadhams 1979: On the statistical distribution of pressure ridges in sea ice. - J. Geophys. Res. 84(C5): 2487-94.

Mock, S.J., A.D. Hartwell & W.D. Hibler III 1972: Spatial aspects of pressure ridge statistics. - J. Geophys. Res. 77(30):5945-53.

Mäkinen, E., A. Keinonen & A. Laine 1976: Ice resistance measurements in ridges with IB APU in the Baltic Sea. - Ocean Engng. 3:267-91.

Palosuo, E. 1975: Formation and structure of ice ridges in the Baltic. - Winter Navigation Research Board, Res. Rep. No 12, 54 p. Helsinki.

- " - 1977: Laser-profilometri jääkenttien tutkimuksessa. [Laser-profilometer in sea ice research .] - In: Helminen, J. (ed.): Geofysiikan päivät Helsingissä 10. - 11.3.1977, pp. 193-96. Geophysical Society of Finland, Helsinki.

- " - 1978: Distribution of sail height and ridge spacing off the coast at Raahe on 23 March 1978. - Unpublished.

- " - & M. Leppäranta 1979: Laser-observationer av packisvallar. [Laser-observations on sea ice ridges .] - XXIV Nordiska Skeppteknіska mötet, pp. 6-8. Helsinki.

Parmerter, R.R. 1975: A model of simple rafting in sea ice. - J. Geophys. Res. 80(15):1948-52.

- " - & M.D. Coon 1972: Model of pressure ridge formation in sea ice. - J. Geophys. Res. 77(33) 6565-75.

Tucker, W. B., III, W.F. Weeks & M.D. Frank 1979: Sea ice ridging over the Alaskan continental shelf. - J. Geophys. Res. 84(C8):4885-97.

Wadhams, P. 1979: A comparison of sonar and laser profiles along corresponding tracks in the Arctic Ocean. - In: Pritchard, R. (ed.): Proc. ICSI/AIDJEX Symp. on Sea Ice Processes and Models, University of Washington.

Weeks, W.F., A. Kovacs & W.D. Hibler III 1971: Pressure ridge characteristics in the Arctic coastal environment. - Proc. 1st Int. Conf. Port Ocean Engng. Arctic conditions, pp. 152-183. Technical University of Norway, Trondheim.

Zubov, N.N. 1945: L´dy Arktiki. [Arctic Ice .] - 360 p. Moscow. Engl. transl. (1963) by U.S. Naval Oceanographic Office and American Meteorological Society, San Diego.

188100421H—100 VAPK

ISBN 951-46-5105-7